Energy Conversion and Management 84 (2014) 282–294

Contents lists available at ScienceDirect

Energy Conversion and Management

journal homepage: www.elsevier.com/locate/enconman

Performance analysis of regenerative organic Rankine cycle (RORC) using the pure working fluid and the zeotropic mixture over the whole operating range of a diesel engine

Jian Zhang [a], Hongguang Zhang [a,*], Kai Yang [a], Fubin Yang [b], Zhen Wang [b], Guangyao Zhao [a], Hao Liu [a], Enhua Wang [a,c], Baofeng Yao [a]

[a] College of Environmental and Energy Engineering, Beijing University of Technology, Pingleyuan No. 100, 100124 Beijing, China
[b] School of Mechanical and Power Engineering, North University of China, 030051 Taiyuan, China
[c] State Key Laboratory of Automotive Safety and Energy, Tsinghua University, Qinghuayuan, 100084 Beijing, China

ARTICLE INFO

Article history:
Received 29 July 2013
Accepted 11 April 2014
Available online 6 May 2014

Keywords:
Performance analysis
Exhaust heat recovery
Regenerative organic Rankine cycle
Zeotropic mixture
Intermediate pressure
Diesel engine

ABSTRACT

A regenerative organic Rankine cycle (RORC) system is designed to recover the exhaust heat of a diesel engine, and the influence of the intermediate pressure (the pressures at which the steam is extracted from the expander) on performance parameters such as net power output, thermal efficiency and mass flow rate of the working fluid are analyzed. The organic working fluids under investigation are R245fa and the zeotropic mixture isopentane/R245fa (in a 0.7/0.3 mol fraction). Based on initial calculations of RORC system performance, the intermediate pressure is set to 1.15 MPa for the RORC system when using isopentane/R245fa (in a 0.7/0.3 mol fraction) as the working fluid, and 1.2 MPa when using R245fa as the working fluid. A performance analysis of the RORC system using the two different working fluids is then conducted over the whole operating range of a diesel engine. The results show that the zeotropic mixture isopentane/R245fa (in a 0.7/0.3 mol fraction) performs better. Finally, a combined diesel engine and RORC system is defined to evaluate the performance improvement of such a combined system over the whole operating range. Results show that, for the combined system, a 10.54% improvement in power output and a 9.55% improvement in fuel economy can be achieved at the engine's rated condition.

1. Introduction

Only about one-third of an engine's fuel combustion energy is converted to mechanical energy, with the remaining energy dissipated in the form of waste heat through the exhaust and the coolant system [1,2]. Therefore, discovering a more efficient and effective way to recover engine waste heat so as to increase engine power output and decrease fuel consumption has become a hot focus of recent research work.

The organic Rankine cycle (ORC) is an effective method of waste heat recovery, and already widely applied in many domains [3–8]. There have been many studies investigating the use of ORC systems to recover and utilize waste heat from internal combustion engines. Vaja and Gambarotta [9] set up three different cycles: a simple cycle using only engine exhaust gas as a thermal source, a simple cycle using exhaust gas and engine cooling water and a regenerated cycle. Their analysis showed that the system achieved a 12% increase in the overall efficiency. Katsanos et al. [10] conducted a theoretical research to analyze the performance of a heavy-duty truck diesel engine equipped with a Rankine bottoming cycle for recovering heat from the exhaust gas. The results revealed that the organic Rankine cycle improved the brake specific fuel consumption by 10.2–8.4% as engine load increased from 25% to 100%. Shu et al. [11] proposed a new dual-loop organic Rankine cycle (DORC) consisting of a high-temperature (HT) cycle and a low-temperature (LT) cycle, recovering the waste heat of the exhaust and the engine coolant as well as the residual heat of the HT cycle. Results showed that the net power output and the exergy efficiency reached 39.91 kW and 48.42%, respectively. Bombarda et al. [12] conducted a thermodynamic performance comparison between a Kalina cycle and an ORC cycle using hexamethyldisiloxane as the working fluid for heat recovery from two diesel engines. Their results indicated that although the obtained useful powers were actually equal in value, the Kalina cycle required a very high maximum pressure in order to obtain high thermodynamic performance. Srinivasan et al. [13] examined the exhaust waste heat recovery potential of an engine using an

* Corresponding author. Tel.: +86 10 67392469; fax: +86 10 67392774.
E-mail address: zhanghongguang@bjut.edu.cn (H. Zhang).

http://dx.doi.org/10.1016/j.enconman.2014.04.036
0196-8904/

Nomenclature

T	temperature (K)
P	pressure (MPa)
s	entropy (kJ/kg K)
h	enthalpy (kJ/kg)
$\dot{I}$	exergy destruction rate (kW)
$\dot{W}$	power output (kW)
$\dot{W}_{net}$	net power output of RORC (kW)
$\dot{m}$	mass flow rate (kg/s)
$\dot{Q}$	heat exchange rate (kW)
$\dot{Q}_{exh}$	available exhaust energy (kW)
$c_{p,exh}$	exhaust specific heat at constant pressure(kJ/kg K)
$bsfc$	brake specific fuel consumption (g/kW h)

Greek letters

ρ	mass density (kg/m^3)
α	fraction of steam extracted (%)
η_t	isentropic efficiency of expander (%)
η_I	thermal efficiency (%)
η_{II}	exergy efficiency (%)
φ_{ep}	improvement of engine power output (%)
φ_{bf}	improvement of engine BSFC (%)

Subscript

cr	critical
L	low-temperature heat source
0	ambient state
exh	exhaust
out	evaporator outlet
1, 2, 2s, 3, 3s, 4, 5, 6, 7, 8	state points in cycle
O	open feed organic fluid heater
t	expander
c	condenser
p1	pump 1
p2	pump 2
e	evaporator
H	high-temperature heat source
in	evaporator inlet
fu	fuel
en	engine
cs	combined system

Acronyms

ORC	organic Rankine cycle
RORC	regenerative organic Rankine cycle
OFOH	open feed organic fluid heater
HFCs	hydrofluorocarbons
HCs	hydrocarbons
GWP	global warming potential
BSFC	brake specific fuel consumption

organic Rankine cycle, and found that the fuel conversion efficiency could be improved by an average of 7 percentage points for all injection timings and loads. Boretti [14] proposed an ORC system to recover the waste heat from the exhaust gas and the coolant of a 1.8 L naturally aspirated gasoline engine. Their results showed that the average improvements of the fuel conversion efficiency all over the map were 3.4% from the exhaust gas and 1.7% from the coolant.

In order to further improve the performance of ORC system, some scholars proposed using the regenerative organic Rankine cycle system. Acar [15] performed energy and exergy analyses for each component in a reheat-regenerative Rankine cycle system. The results demonstrated that the thermal efficiency of the cycle increased when using regeneration. Mago et al. [16] analyzed the performance of regenerative organic Rankine cycles using dry organic fluids and compared the regenerative ORC with the basic ORC using a combined first and second law analysis. Their results showed that the regenerative ORC produced a higher efficiency compared with the basic ORC. Wang et al. [17] evaluated the performance of five different types of ORC, showing that the exergy destruction rate of the regenerative ORC was the lowest.

Currently, most research works put a particular emphasis on contrasting the thermodynamic performance of regenerative ORC systems with that of other ORC types. However, few of these works have investigated the influence of parameters such as intermediate pressure in a regenerative ORC system on system performance. Moreover, most scholars take only one, or at most a few, operating points into account when studying an engine waste heat recovery system. In fact, few scholars have investigated the performance of regenerative ORC systems over the whole operating range of an internal combustion engine. Considering the aforementioned cases, in this paper we analyze the exhaust characteristics from a six-cylinder diesel engine over its whole operating range by engine experiments, and devise a regenerative organic Rankine cycle (RORC) system using R245fa and isopentane/R245fa (in a 0.7/0.3 mol fraction) as working fluids. We also study the effects of intermediate pressure on the thermodynamic performance of the RORC system, then analyze and compare the performance of the RORC system using the two different working fluids. Finally, we develop a combined engine and RORC system, and the dynamics performance and fuel economy of the combined system are analyzed and compared with that of the engine itself.

2. RORC system design

2.1. Description of the RORC system

In this paper, a set of devices for regeneration are added to an ORC system to implement a regenerative organic Rankine cycle (RORC) system. The key components of the RORC system consist of an evaporator, an expander, a generator, a condenser, a reservoir, two pumps, and an open feed organic fluid heater (OFOH). The schematic diagram of the RORC system is shown in Fig. 1: the blue solid lines denote the air intake path; the red and yellow solid lines represent the exhaust path before and after the heat exchange in the evaporator, respectively; the red dashed lines indicate the gas state working fluid; the dark blue dashed lines show the low-temperature liquid state working fluid (i.e., the outlet temperature of the condenser); and the light blue dashed lines indicate the medium temperature liquid state working fluid (i.e., the outlet temperature of the OFOH). The RORC system operates according to the following process. First, pump 2 pressurizes the saturated liquid state working fluid and sends it into the evaporator, where the working fluid absorbs the heat from the engine exhaust and turns into high-temperature and high-pressure saturated steam. This steam then enters the expander to rotate the shaft. When the steam pressure drops to an intermediate pressure, part of the steam is extracted and routed to the OFOH for regeneration, while the rest of the steam continues to expand to produce more work until the pressure drops to the condensing pressure. Then the steam enters the condenser, where it condenses into a saturated liquid state and flows into the reservoir. Pump 1 then pressurizes the liquid and sends it to the OFOH to exchange heat with the

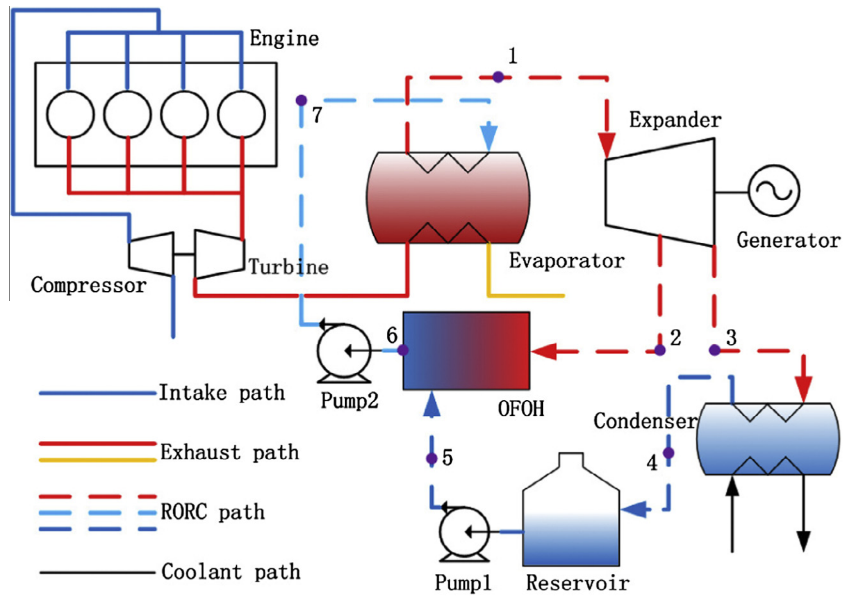

Fig. 1. Schematic diagram of the RORC system.

steam extracted from the expander. Finally, the working fluid in a saturated liquid state is pressurized by pump 2 to the evaporating pressure and sent to the evaporator, thus the whole cycle is completed.

The heat exchanger employed for this research is a finned-tube heat exchanger, which has a larger heat transfer area compared with a shell-and-tube heat exchanger to improve the heat transfer between the working fluid and the engine exhaust. Moreover, a finned-tube heat exchanger has a lower internal flow resistance compared to a plate heat exchanger, so friction loss is decreased. Generally speaking, the working fluid in the tube of a finned-tube heat exchanger experiences three zones: the preheated zone, the two-phase zone, and the superheated zone, as shown in Fig. 2. In the preheated zone, the working fluid is heated from a sub-cooled state 2 (point 2 in Fig. 2) to a saturated liquid state 3 (point 3 in Fig. 2). In the two-phase zone, the working fluid turns into a saturated gas state 4 (point 4 in Fig. 2). In the superheated zone, the working fluid continues to absorb waste heat from the engine exhaust and changes from state 4 to a superheated gas state 5 (point 5 in Fig. 2) [18].

As the key power output component in the waste heat recovery system, the expander plays a crucial role in the recovery performance of the entire system. Currently, expanders commonly used in ORC waste heat recovery systems are primarily turbines [19,20], reciprocating piston expanders [21,22], or screw expanders [23,24]. In general, each type of expander has both advantages and disadvantages. While turbines are relatively lightweight and have a high efficiency, they are expensive, have a low efficiency in off-design conditions, and cannot make use of a two-phase working fluid. Reciprocating piston expanders have a relatively high pressure ratio, but have so many moving parts that the weight of a reciprocating piston expander is too high. Screw expanders can tolerate a two-phase state during the expansion process, but have strict lubrication requirements and are difficult to manufacture and seal.

Taking these expander issues into consideration, the expander selected for this paper is a single screw expander invented at Beijing University of Technology, a photo of which is shown in Fig. 3. There are three working processes in the working cycle of this single screw expander: steam admission, steam expansion, and steam discharge. When the expander begins to work, the inlet steam pushes the spinning rotor with a certain pressure, spinning the gaterotors with the rotor. The inlet steam expands in the closed volume formed by the spiral groove, the gaterotor tooth, and the body shell as the rotor rotates. During the expansion process, compressed steam in the closed volume expands, leading to a decrease in both temperature and pressure that determines the output power [25].

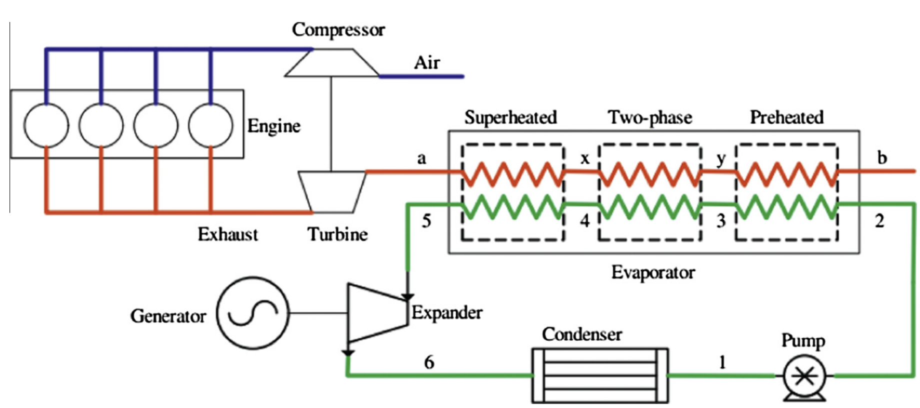

Fig. 2. Schematic of the heat transfer process of the evaporator.

Fig. 3. The single screw expander.

The OFOH in the regeneration process is essentially a direct contact heat exchanger. In an ideal regeneration process, the system extracts some working fluid steam that has not completely expanded from the expander and routes the steam to the OFOH, where it mixes with the condensed working fluid. This mixture leaves the OFOH as a saturated liquid at the intermediate pressure. The thermodynamic performance of the waste heat recovery system can be effectively improved through such a regeneration process. One of our published papers [17] has demonstrated that a RORC system can achieve higher thermal and exergy efficiencies compared to a simple ORC system, and other researchers [16] have arrived at similar conclusions.

2.2. Organic working fluids selection

Selection of a proper organic working fluid is crucial to the performance of an ORC system. Currently, the working fluids selected by most researchers fall into several categories: hydrofluorocarbons (HFCs), hydrocarbons (HCs) and their mixtures.

In some studies, R245fa has performed well as the working fluid in ORC systems [26,27], while isopentane is extensively used in the low temperature waste heat recovery field [28,29]. Despite their utility, both of these working fluids have some disadvantages: R245fa possesses a relatively high global warming potential (GWP) value, and isopentane is too flammable and explosive to be used in engine exhaust waste heat recovery systems. However, according to the study by Garg et al. [30], a 0.7/0.3 mol fraction of isopentane/R245fa mixture allows the R245fa to effectively inhibit the flammability of the isopentane and the isopentane to dramatically decrease the GWP value of R245fa.

Therefore, in this paper we use R245fa and a mixture of isopentane and R245fa in a 0.7/0.3 mol fraction (marked as isopentane/R245fa) as working fluids to study the thermodynamic performance of our RORC system and to compare the suitability of the two different working fluids. The main properties of isopentane, R245fa, and isopentane/R245fa are listed in Table 1. The thermodynamic properties were calculated using REFPROP [31], while the GWP values are quoted from Ref. [30].

Fig. 4 is the *T–s* diagram of the two working fluids (R245fa and isopentane/R245fa), which shows that both working fluids are dry fluids. Based on Ref. [16], a superheat state cannot obviously improve the thermal efficiency of a RORC system when using dry fluids. Therefore, in the calculations performed in this paper, the working fluids at the outlet of the evaporator are in a saturated gas state, and the superheat is not adopted.

3. Thermodynamic model of the RORC system

Fig. 5 is the *T–s* diagram of the RORC system using isopentane/R245fa as the working fluid. In the figure, Process 1–3s is the isentropic expansion process, while Process 1–3 is the actual expansion process. The regeneration process corresponds to Processes 2–6 and 5–6, while Process 3–4 is the isobaric condensing process of the working fluid in the condenser. Processes 4–5 and 6–7 are the compression process of the working fluid in the pumps, and Process 7–1 is the isobaric evaporating process of the working fluid in the evaporator. Since isopentane/R245fa is a zeotropic mixture, there exists a phenomenon called "temperature glide" in both the isobaric evaporating process and the isobaric condensing process, which can be seen in the figure. That is, a certain difference exists between the bubble point temperature and the dew point temperature at the same pressure.

Based on the first and second laws of thermodynamics, a numerical model for each component in the working process of the RORC system is developed. Assumptions for the thermodynamic calculations of the RORC system are the following:

(1) Any pressure and heat loss of the working fluid in the pipelines, evaporator, condenser, and OFOH are ignored.
(2) The temperature of the low-temperature heat source T_L and the ambient temperature T_0 are set to 308.15 K and 303.15 K respectively, while the ambient pressure P_0 is set to 0.1 MPa.
(3) In order to avoid low-temperature corrosion [32], the exhaust temperature at the outlet of the evaporator $T_{exh,out}$ is set to 383.15 K.
(4) The inlet pressure of the expander is set to 2.4 MPa and the expansion ratio of the expander is 6.
(5) The mechanical efficiency of pumps 1 and 2 are both set to 0.8, while the mechanical efficiency and isentropic efficiency of the expander are set to 0.8 and 0.85, respectively.

When the RORC system is running smoothly and correctly, the thermodynamic model follows the series of calculations described in Sections 3.1 to 3.6.

3.1. Open feed organic fluid heater (corresponding to Processes 2–6 and 5–6 in Fig. 5)

In the OFOH, steam extracted from the expander is mixed with liquid working fluid after condensation. The fraction of steam extracted is calculated with the equation below:

Table 1
Properties of the three working fluids.

Working fluids	T_{cr} (K)	P_{cr} (MPa)	ρ (kg/m^3)	Molecular mass (kg/kmol)	GWP
Isopentane	460.35	3.38	236.00	72.15	10
R245fa	427.16	3.65	516.08	134.05	1020
Isopentane/R245fa	450.39	3.98	310.76	90.72	459

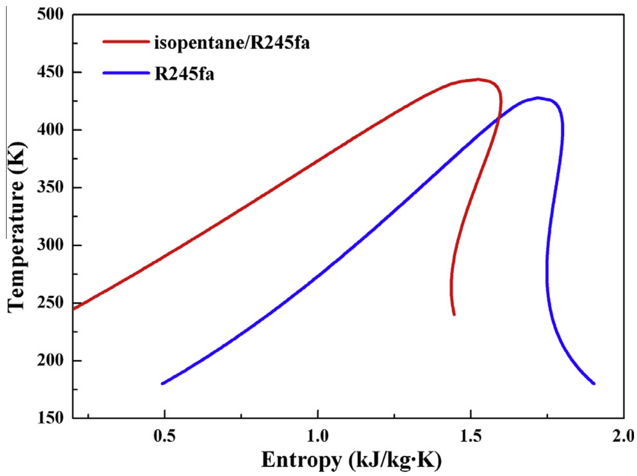

Fig. 4. *T–s* diagram of the two working fluids.

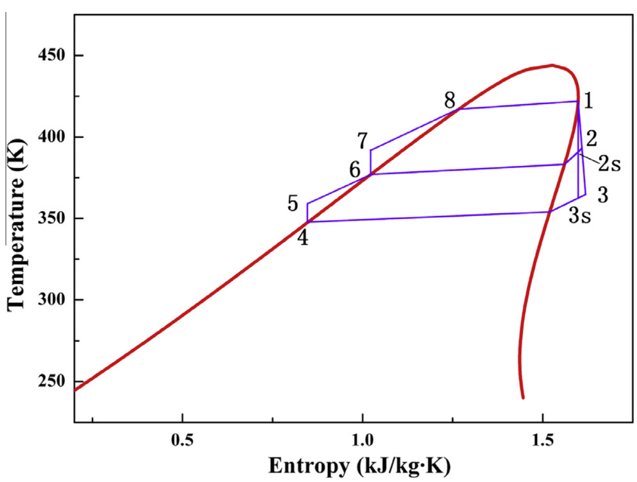

Fig. 5. *T–s* diagram of the RORC system using isopentane/R245fa.

$$\alpha = \frac{h_6 - h_5}{h_2 - h_5} \tag{1}$$

The exergy destruction rate of the OFOH is:

$$\dot{I}_o = T_0\dot{m}[s_6 - \alpha s_2 - (1-\alpha)s_5] \tag{2}$$

3.2. Expander (corresponding to Process 1–3 in Fig. 5)

The isentropic efficiency of the expander is:

$$\eta_t = \frac{h_1 - h_3}{h_1 - h_{3s}} \tag{3}$$

The power output of the expander is:

$$\dot{W}_t = \dot{m}[(h_1 - h_2) + (1-\alpha)(h_2 - h_3)] \tag{4}$$

The exergy destruction rate of the expander is:

$$\dot{I}_t = T_0\dot{m}[(s_2 - s_1) + (1-\alpha)(s_3 - s_2)] \tag{5}$$

3.3. Condenser (corresponding to Process 3–4 in Fig. 5)

The heat exchange rate of the condenser is:

$$\dot{Q}_c = \dot{m}(1-\alpha)(h_3 - h_4) \tag{6}$$

The exergy destruction rate of the condenser is:

$$\dot{I}_c = T_0(1-\alpha)\dot{m}\left[(s_4 - s_3) - \frac{(h_4 - h_3)}{T_L}\right] \tag{7}$$

3.4. Pump (corresponding to Processes 4–5 and 6–7 in Fig. 5)

The shaft work consumed by pump 1 is:

$$\dot{W}_{p1} = \dot{m}(1-\alpha)(h_5 - h_4) \tag{8}$$

The shaft work consumed by pump 2 is:

$$\dot{W}_{p2} = \dot{m}(h_7 - h_6) \tag{9}$$

Note that because the irreversible loss of the pump is relatively small, it is ignored.

3.5. Evaporator (corresponding to the Process 7–1 in Fig. 5)

The heat exchange rate of the evaporator is determined by:

$$\dot{Q}_e = \dot{m}(h_1 - h_7) \tag{10}$$

The exergy destruction rate of the evaporator is:

$$\dot{I}_e = T_0\dot{m}\left[(s_1 - s_7) - \frac{(h_1 - h_7)}{T_H}\right] \tag{11}$$

Here, T_H is the temperature of the high-temperature heat source i.e., the mean temperature of the engine exhaust and is calculated using

$$T_H = \frac{T_{exh,in} - T_{exh,out}}{\ln\left(\frac{T_{exh,in}}{T_{exh,out}}\right)} \tag{12}$$

3.6. The performance parameters of the RORC system

The net power output is:

$$\dot{W}_{net} = \dot{W}_t - (\dot{W}_{p1} + \dot{W}_{p2}) \tag{13}$$

The thermal efficiency is:

$$\eta_I = \frac{\dot{W}_{net}}{\dot{Q}_e} \times 100\% \tag{14}$$

The exergy efficiency can be expressed as:

$$\eta_{II} = \frac{\dot{W}_{net}}{\dot{Q}_e(1 - T_L/T_H)} \times 100\% \tag{15}$$

Note that Eq. (12) is derived from Ref. [33], while all remaining equations from Eqs. (3)–(15) come from Ref. [17]. The thermodynamic parameters of each state point are shown in Table 2.

4. Engine performance and engine exhaust

The engine used in this study is a six-cylinder in-line turbocharged diesel engine equipped with a common rail fuel injection system. The engine performance test was carried out according to Ref. [1], and the performance of the diesel engine including the variation of the exhaust energy over the whole operating range is analyzed based on the test data. In the test process, the engine speed varies from 700 r/min to 2200 r/min at intervals of 100 r/min, with nine different load conditions tested at each engine speed.

Table 2
The thermodynamic parameters of each state point of the RORC system.

Working fluids	State point	Pressure (MPa)	Temperature (K)	Enthalpy (kJ/kg)	Entropy (kJ/kg K)
Isopentane/R245fa	1	2.4	421.9714	508.1216	1.5983
	2	1.15	392.3578	491.8799	1.6056
	2s	1.15	390.8489	489.0137	1.5983
	3	0.4	364.7384	465.3412	1.6191
	3s	0.4	360.0594	457.7917	1.5983
	4	0.4	331.9239	173.4255	0.7533
	5	1.15	332.3030	174.4319	0.7533
	6	1.15	377.0266	269.7355	1.0220
	7	2.4	378.1080	271.6247	1.0220
	8	2.4	417.0972	368.9082	1.2664
R245fa	1	2.4	404.3813	487.9742	1.7995
	2	1.2	374.8399	478.1920	1.8041
	2s	1.2	373.5166	476.4658	1.7995
	3	0.4	343.5355	460.8176	1.8136
	3s	0.4	338.9852	456.0253	1.7995
	4	0.4	328.1455	273.2450	1.2431
	5	1.2	328.5162	273.8831	1.2431
	6	1.2	370.8068	336.1054	1.4210
	7	2.4	371.7944	337.1892	1.4210
	8	2.4	404.3813	392.6677	1.5639

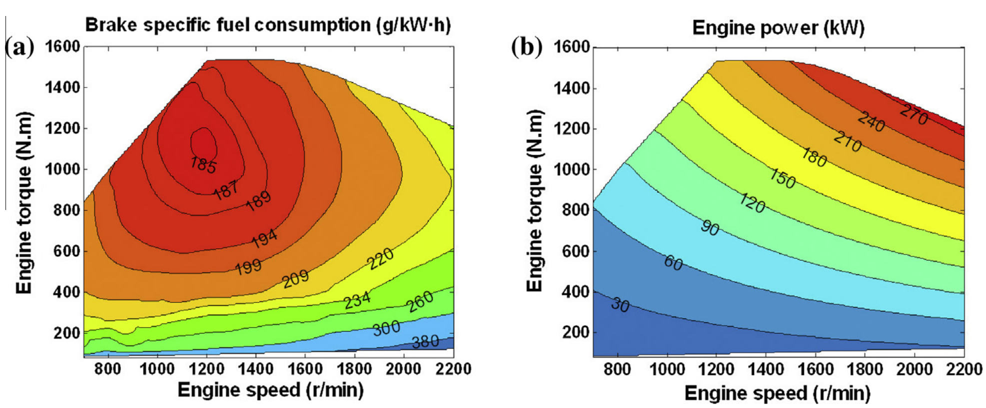

Fig. 6. Performance MAPs of the diesel engine.

4.1. Performance of the diesel engine

The performance MAPs of the diesel engine are illustrated in Fig. 6. The variation in brake specific fuel consumption (BSFC) over the whole load and speed range is shown in Fig. 6(a), which indicates that the BSFC is relatively low in the engine's medium- and high- load regions. When the engine speed is 1200 r/min and the engine load is 1130 N m, the BSFC reaches a minimum value of 184.54 g/kW h. On the other hand, the BSFC is relatively high in the engine's low-load regions, particularly in the high-speed and low-load regions. The MAP of the power output of the diesel engine is given in Fig. 6(b), which shows that the maximum torque appears at engine speeds of 1200–1600 r/min. Moreover, engine power output gradually increases as engine's speed and load increase. At the engine's rated condition, the power output of the engine reaches a maximum value of 279 kW.

The characteristics of the diesel engine exhaust are shown in Fig. 7, where Fig. 7(a) denotes the variation of the exhaust temperature with the diesel engine's speed and load. As can be seen in the diagram, the exhaust temperature varies slightly with engine speed, but increases dramatically with engine load. The reason for this difference is that the combustion energy increases as the mass of fuel injection increases in high engine load regions. At the engine's rated condition, the engine exhaust temperature is 819 K. The variation of diesel engine exhaust mass flow rate with the engine's speed and load is shown in Fig. 7(b). The diagram shows that variation of the exhaust mass flow rate is more obvious with changes in engine speed than with changes in engine load. The reason for this is that the exhaust mass flow rate of a diesel engine is primarily dependent on the mass flow rate of intake air, which increases significantly with the increasing engine speed. The exhaust mass flow rate reaches a maximum of 0.48 kg/s at the engine's rated condition.

4.2. Engine available exhaust energy evaluation

Using test data of engine exhaust temperature and mass flow rate, the available exhaust energy (i.e., the heat transfer rate between the engine exhaust and the working fluid in the evaporator) can be calculated with

$$\dot{Q}_{exh} = c_{p,exh}\dot{m}_{exh}(T_{exh,in} - T_{exh,out}) \tag{16}$$

where $c_{p,exh}$ is the exhaust specific heat at constant pressure. The variation of the specific heat of the exhaust at constant pressure as a function of exhaust temperature is shown in Fig. 8.

The MAPs of the diesel engine available exhaust energy is shown in Fig. 9. Note that, as the engine's speed and load increase, the available exhaust energy also increases. At the engine's rated condition, the available exhaust energy is 239 kW. By contrasting Figs. 9 and 6(b), it can be concluded that the diesel engine's available exhaust energy increases in an approximately linear fashion

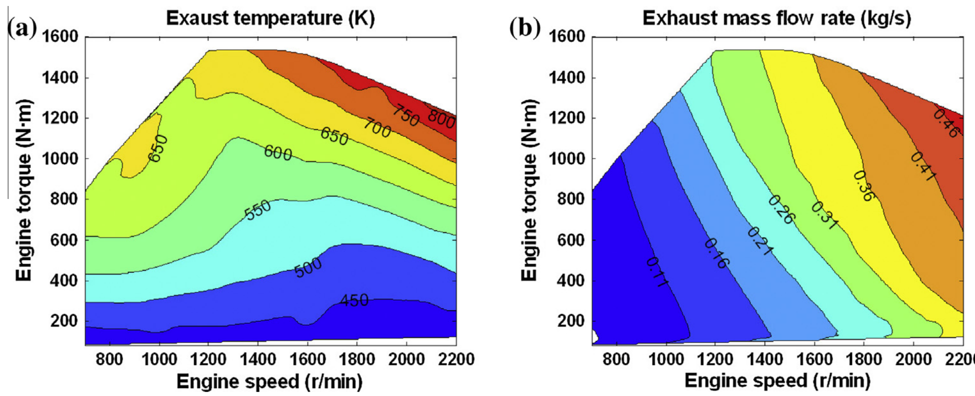

Fig. 7. Characteristics MAPs of the engine exhaust.

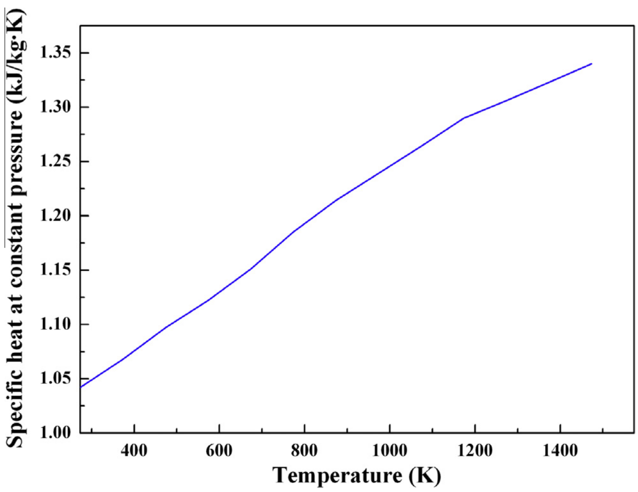

Fig. 8. The exhaust specific heat at constant pressure.

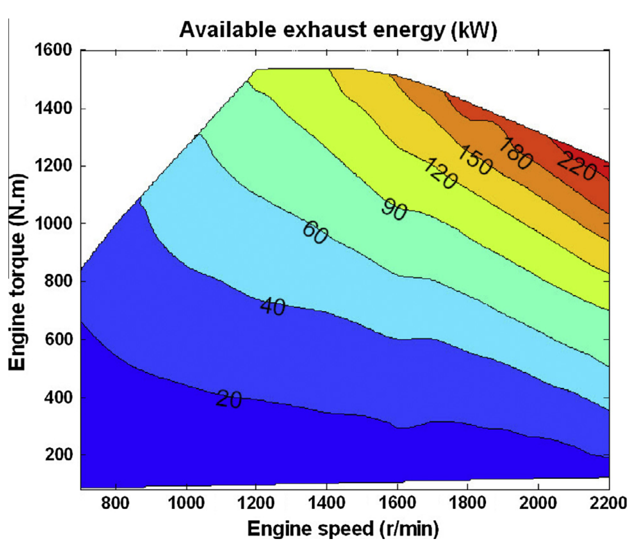

Fig. 9. Available exhaust energy of the diesel engine.

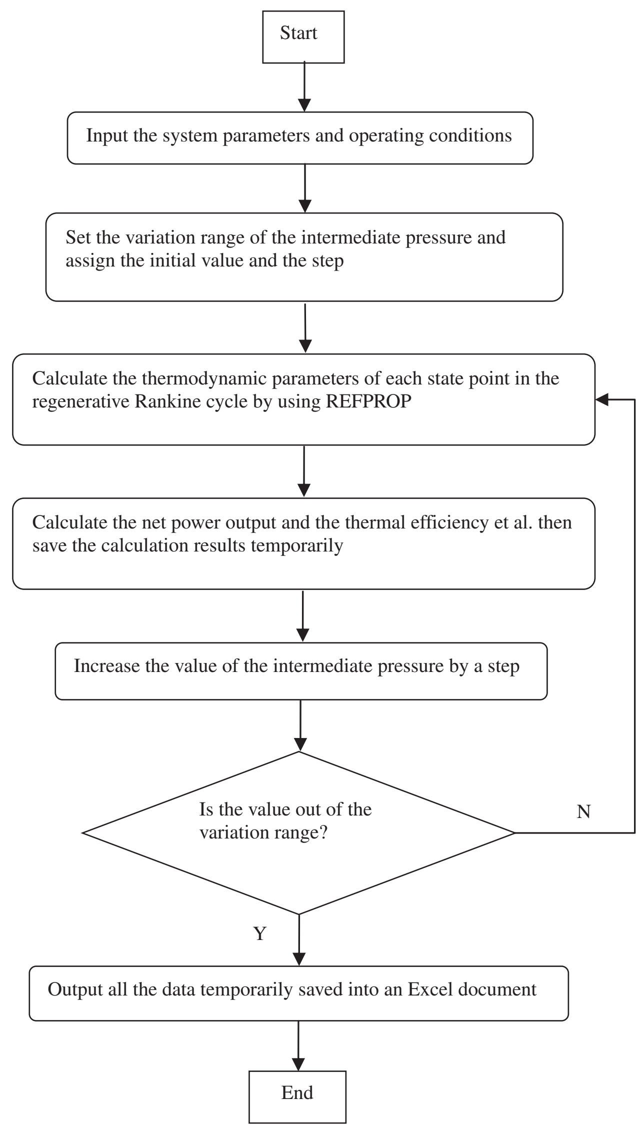

Fig. 10. Flow chart describing the algorithm for simulating the effect of the intermediate pressure in the proposed RORC system.

with engine power output, and the value of the available exhaust energy nearly equals that of the power output. This proves that there is a large potential amount of energy that can be recovered from engine exhaust.

5. Results and analysis

Based on the thermodynamic model of the RORC system, calculation programs were run in MATLAB 7.12 [34]. The effects of the

intermediate pressure in the RORC system on the system performance were analyzed. Fig. 10 provides a flow chart of the simulation program. Over the whole operating range of the diesel engine, simulations were conducted for both working fluids, and the performance of the RORC system was analyzed and compared. Based on the results of the effect of the intermediate pressure, we chose isopentane/R245fa as the working fluid for evaluating the performance of the combined engine and RORC system. The corresponding flow chart describing these simulations is given in Fig. 11.

5.1. Effect of the intermediate pressure on RORC system performance

The intermediate pressure and the fraction of steam extracted are two crucial parameters for describing a RORC system: the intermediate pressure indicates the pressure at which the steam is extracted from the expander, while the fraction of steam extracted determines how much working fluid is needed to be extracted from the expander. These two parameters must be in the correct ratio in order to ensure that the working fluid is at a saturated liquid state at the outlet of the OFOH. The variation in fraction of steam extracted with the variation in intermediate pressure for the RORC system using the two different working fluids is shown in Fig. 12. As can be seen in the diagram, the fraction of steam extracted increases as the intermediate pressure increases. Moreover, the fraction of steam extracted by the RORC system using isopentane/R245fa is slightly more than the steam extracted

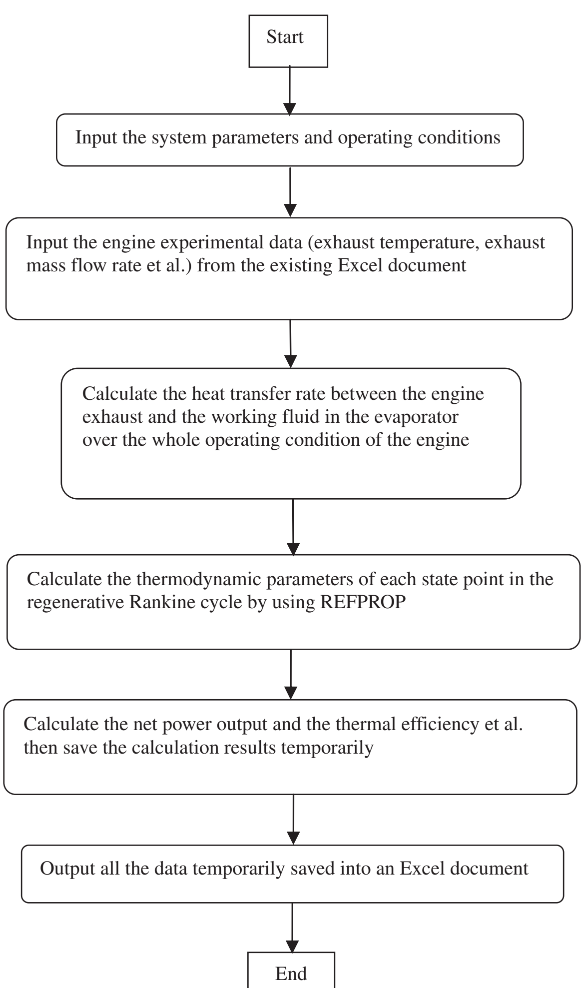

Fig. 11. Flow chart describing the algorithm for simulating the proposed combined system.

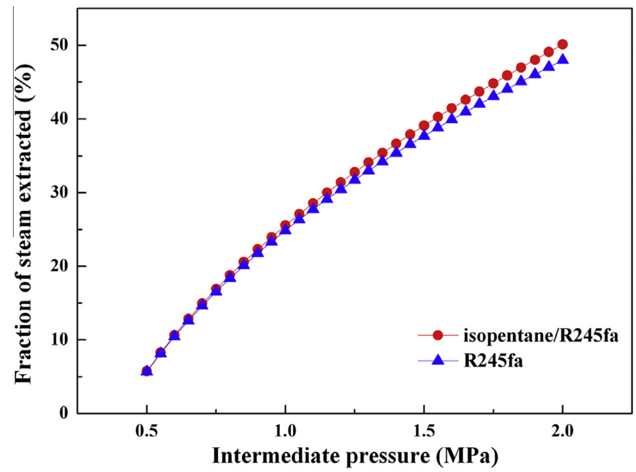

Fig. 12. Relationship between the fraction of steam extracted and the intermediate pressure.

using R245fa at the same intermediate pressure, a difference that becomes more obvious as the intermediate pressure increases.

The variation of the net power output with the intermediate pressure of the RORC system using the two different working fluids is shown in Fig. 13. The graph shows that at a certain intermediate pressure, the net power output of the RORC system using isopentane/R245fa is higher than the output using R245fa, and the difference between them increases gradually with the increase of the intermediate pressure and then decreases after reaching the maximum value around the intermediate pressure 1.2 MPa. Over the entire variation range of the intermediate pressure, the net power output of the RORC system using the two working fluids first increases and then decreases, which shows that an appropriate intermediate pressure is beneficial for increasing the net power output of the RORC system.

The variation of the thermal efficiency with the intermediate pressure of the RORC system using the two different working fluids is shown in Fig. 14. As seen in the diagram, the thermal efficiency of the RORC system using isopentane/R245fa is higher than the same system using R245fa at equivalent intermediate pressures. Furthermore, in the process of calculating, the amount of the exhaust heat absorbed by the working fluids is constant, so the variation tendency of the thermal efficiency of the RORC system is accordant with that of the net power output of the RORC

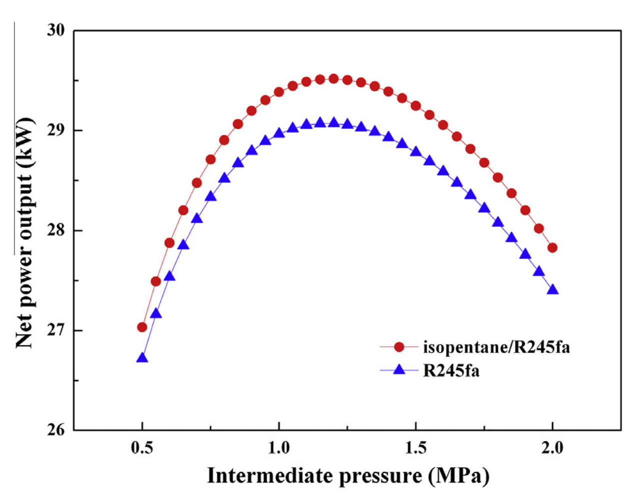

Fig. 13. Variation of the net power output with the intermediate pressure.

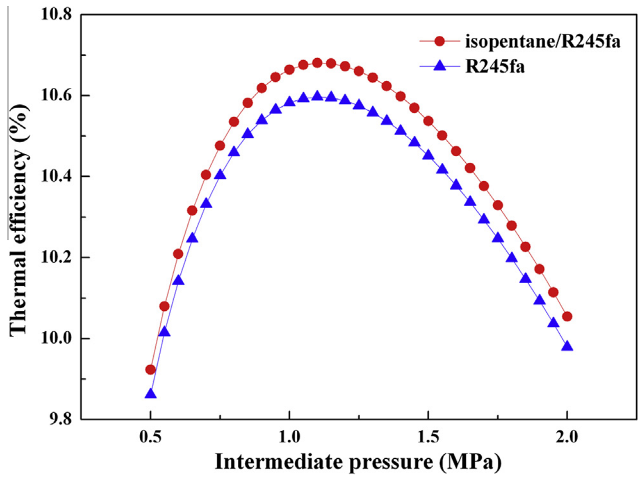

Fig. 14. Variation of the thermal efficiency with the intermediate pressure.

system. The thermal efficiency of the RORC system increases first and then decreases with the increase of the intermediate pressure.

Fig. 15 illustrates the change in working fluid mass flow rate of the RORC system as the intermediate pressure changes using the two different working fluids. It can be seen from the diagram, when taking the isopentane/R245fa as working fluid, the mass flow rate needed by the RORC system is smaller than the case using R245fa. Moreover, as the intermediate pressure increases, the mass flow rate of both the two working fluids increases as well. The reason for this trend is that, at high intermediate pressure, the steam extracted has a high enthalpy value due to incomplete expansion leading to a decrease in enthalpy difference between the inlet and the outlet of the evaporator and thus a increase in the mass flow rate of the working fluid.

Fig. 16 shows the variation of the exergy efficiency with the intermediate pressure of the RORC system using the two different working fluids. As seen, with the increase of the intermediate pressure, the variation tendency of the exergy efficiency is similar to that of the thermal efficiency which increases first and then decreases. Furthermore, the RORC system using isopentane/R245fa has a higher exergy efficiency than the system using R245fa for a given intermediate pressure, with the largest difference occurring in the medium intermediate pressure range of 0.9–1.2 MPa.

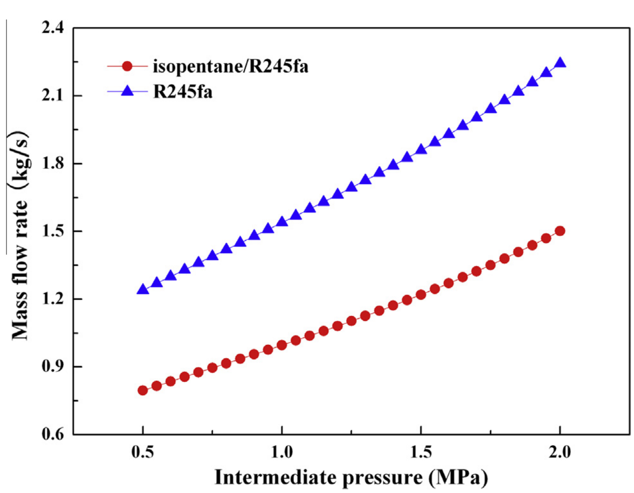

Fig. 15. Variation of the mass flow rate of the working fluid with the intermediate pressure.

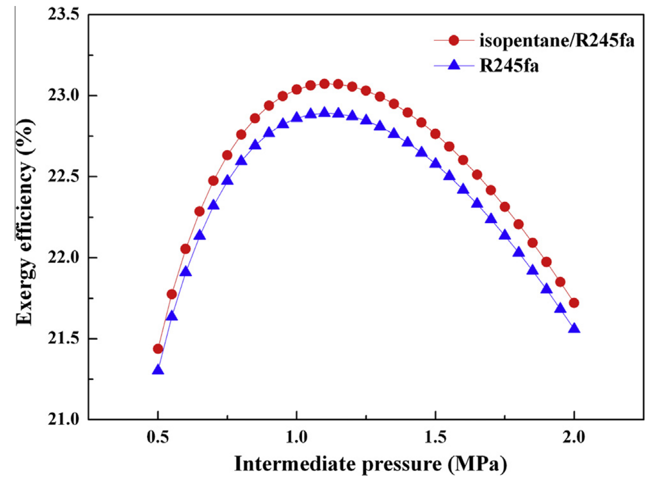

Fig. 16. Variation of the exergy efficiency with the intermediate pressure.

The variation of the exergy destruction rate of the RORC system using the two working fluids is shown in Fig. 17. It can be observed that the system exergy destruction rate first decreases then increases. This outcome fits the result shown in Fig. 16, as an increase in exergy efficiency means a decrease in exergy destruction rate.

5.2. RORC system performance analysis over the whole operating range of the diesel engine

Based on the above analysis about the variation of the performance with the intermediate pressure of the RORC system using the two different working fluids, the intermediate pressure of the RORC system when using isopentane/R245fa as working fluid was set to 1.15 MPa, while the intermediate pressure was set to 1.2 MPa when using R245fa. Then the performance of the RORC system using the two different working fluids over the engine whole operating range was analyzed and compared.

Fig. 18 illustrates how the net power output of the RORC system using the two different working fluids changes over the engine whole operating range. To clearly compare the net power output of the RORC system using different working fluids, the distribution tendency of the contour lines in Fig. 18 are consistent, while the values they represent are different. It can be seen in the diagrams, with the increase of the engine's speed and load, the net power

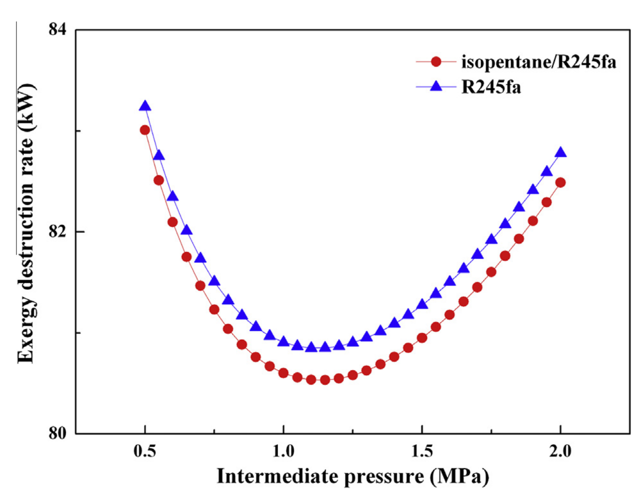

Fig. 17. Variation of the exergy destruction rate with the intermediate pressure.

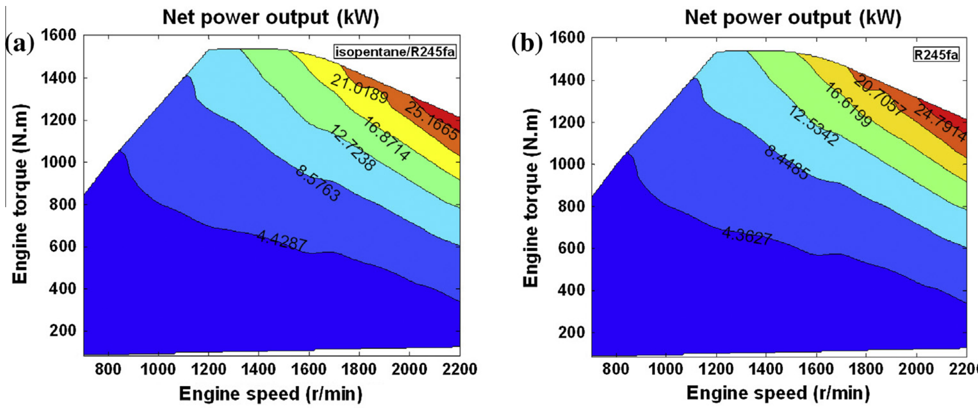

Fig. 18. Net power output of the RORC system using the two working fluids.

output of the RORC system for the two working fluids shows an increasing trend. At the engine's rated condition, the net power output for isopentane/R245fa reaches a maximum of 29.5118 kW, and a maximum of 29.0720 kW for R245fa. Furthermore, by comparing Fig. 18(a and b), we can see that the net power output for isopentane/R245fa is larger than that of R245fa for a given set of engine operating conditions, and the difference between the net power outputs increases with both increasing engine's speed and load.

The MAPs of the mass flow rate for the two working fluids over the engine whole operating range are shown in Fig. 19. As can be seen, with the increase of the engine's speed and load, the mass flow rate of each working fluid increases. The reason for this result is that an increase in either engine speed or load also increases the available exhaust energy (as shown in Fig. 9), so it follows that the working fluid mass evaporated by the exhaust also increases. Furthermore, the mass flow rate for isopentane/R245fa is smaller than that of R245fa at the same engine operating conditions. At the engine's rated condition, the mass flow rate for the two working fluids reaches a maximum of 1.0597 kg/s for isopentane/R245fa and 1.6620 kg/s for R245fa, respectively. Besides, a comparison between Figs. 19 and 18 shows that the change trend of mass flow rate is similar to that of the change trend of net power output. The reason for this similarity is that the RORC system parameters—

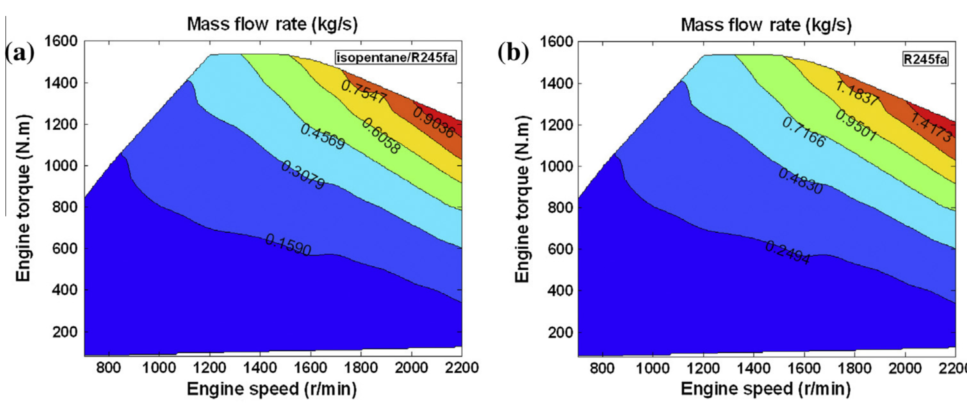

Fig. 19. Mass flow rate of the two working fluids.

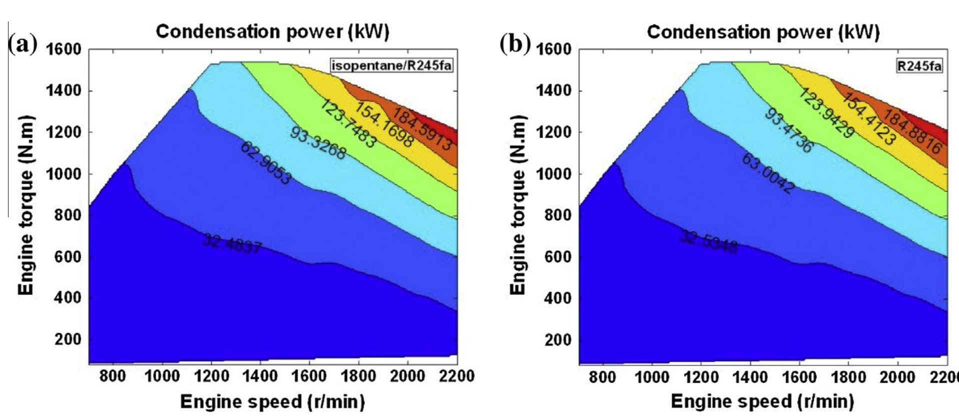

Fig. 20. Condensation power of the RORC system using the two working fluids.

including expander efficiency, intermediate pressure, and the thermodynamic parameters of pressure, temperature, and specific enthalpy of the working fluid—are known quantities for the above calculations, making the net power output simply a function of the mass flow rate. Therefore, any change in the mass flow rate will be reflected in the net power output.

The condensation power of the RORC system using the two different working fluids over the whole operating range of the diesel engine is shown in Fig. 20. Under laboratory conditions we choose to use a water cooling tower to reject the heat power to the ambient atmosphere. The cooling water, as the low-temperature heat source of the condenser in the RORC system, flows into the condenser by way of the cooling tower and a water pump to cool the working fluid steam down to a saturated liquid, then returns to the cooling tower to begin the next cycle. Note that if the RORC system is applied to a heavy-duty vehicle, an air-cooled radiator could be used to provide this cooling in a manner similar to how an engine coolant system functions.

The variation of the exergy efficiency of the RORC system using the two different working fluids with the engine's speed and load is shown in Fig. 21. In the low-speed and low-load regions of the engine, the exergy efficiency of the RORC system is higher than in the high-speed and high-load regions. This is because, under the engine high-speed and high-load working conditions, the mean temperature of the engine exhaust increases, leading to the decrease of the exergy efficiency. Moreover, comparing the graphs in Fig. 21(a and b) makes it clear that the RORC system using isopentane/R245fa as working fluid has a higher exergy efficiency for a given engine operating condition.

Fig. 22 indicates the MAPs of the exergy destruction rate of the RORC system using the two different working fluids over the engine whole operating range. Note that the exergy destruction rate of the RORC system shows an increasing trend for both of the working fluids as engine's speed and load increase. This increase occurs because the heat of the exhaust dramatically increases in the engine's high-speed and high-load regions, increasing the temperature difference between the exhaust and the working fluid in the evaporator, causing an increase in irreversible loss of RORC system, and leading to an increase of the exergy destruction rate. Moreover, comparing the results of Fig. 22(a and b) shows that the RORC system using isopentane/R245fa has a

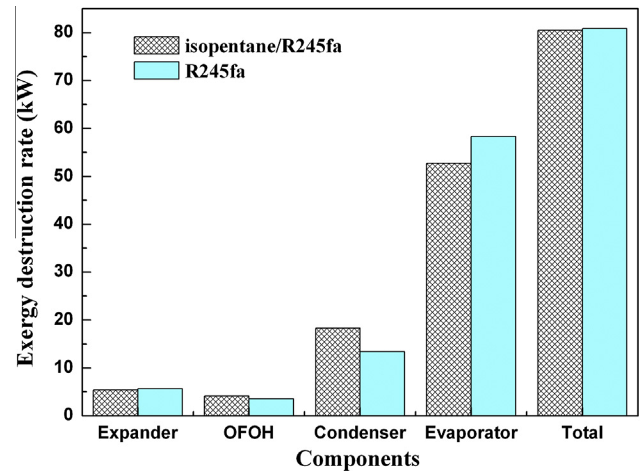

Fig. 23. Exergy destruction rate of each component and for the total RORC system under the engine's rated condition.

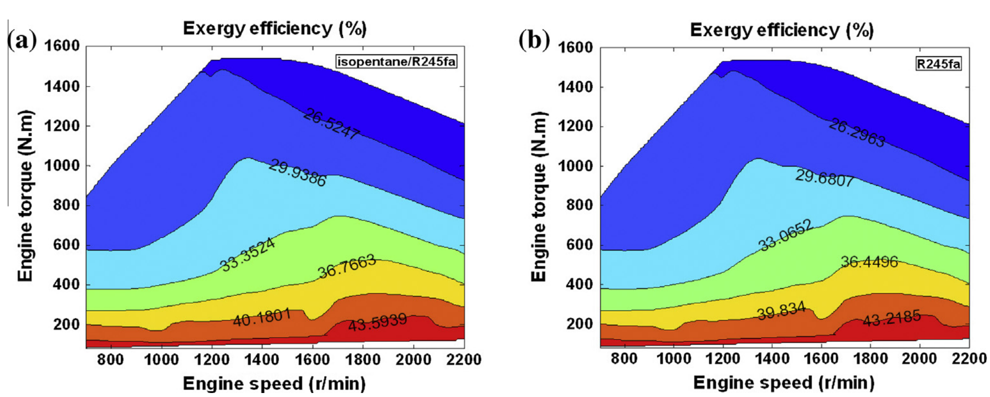

Fig. 21. Exergy efficiency of the RORC system using the two working fluids.

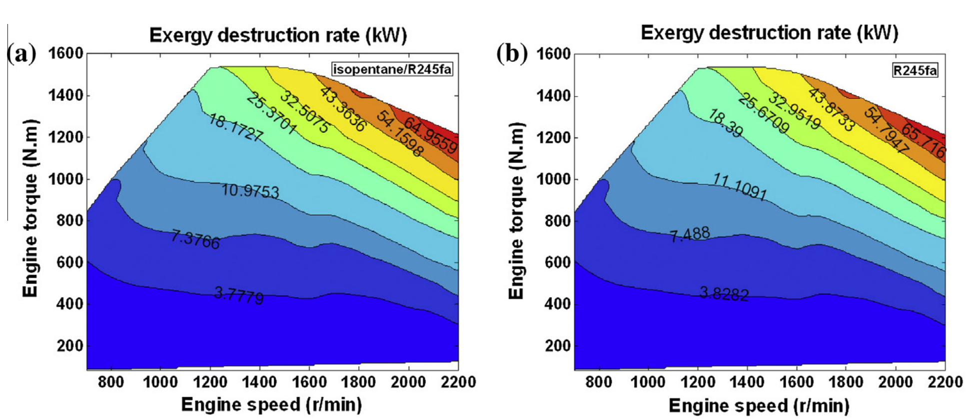

Fig. 22. Exergy destruction rate of the RORC system using the two working fluids.

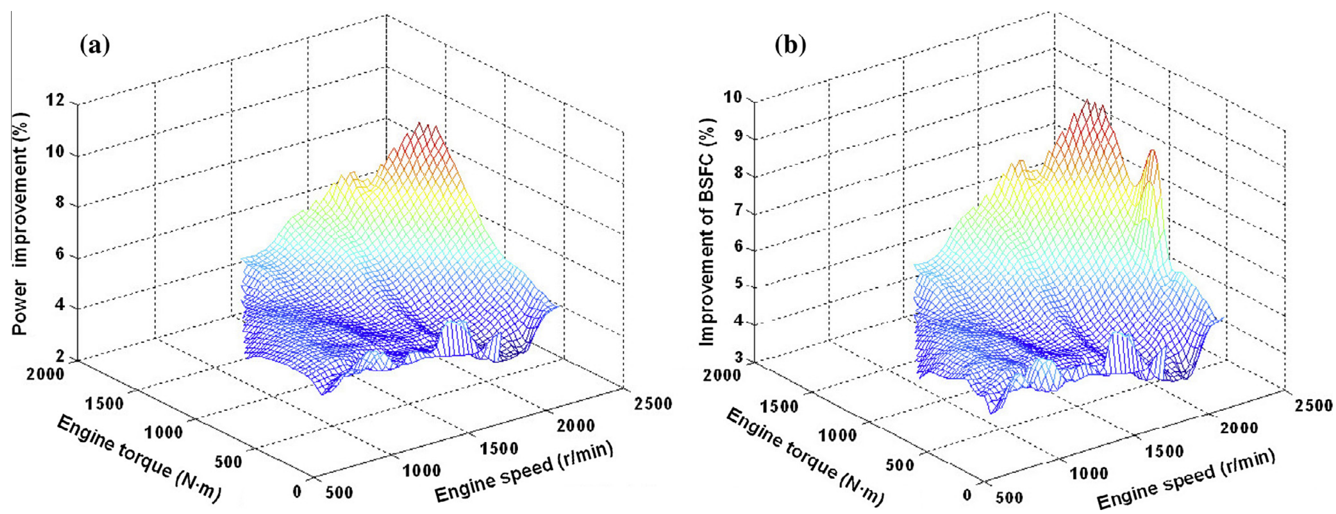

Fig. 24. Performance of the combined system.

lower exergy destruction rate for a given engine operating conditions. This result is due to the phenomenon of "temperature glide" in the evaporating and condensing processes for zeotropic mixtures, which decreases the heat-transfer temperature difference during those processes, and thus decreases the exergy destruction rate.

The exergy destruction rate of each component and for the total RORC system under the engine's rated condition is presented in Fig. 23. The figure shows that the evaporator is the component that possesses the highest exergy destruction rate in the RORC system, no matter which working fluid is used.

Based on all of the results described above, we can conclude that the RORC system using isopentane/R245fa as the working fluid displays superior thermodynamic properties to the same system using R245fa as the working fluid, and does so over the diesel engine whole operating range.

In order to optimize the power system as a whole and comprehensively evaluate the improvement in overall power output and engine fuel economy, the novel concept of a "combined engine and RORC system" was defined. In the combined system, the diesel cycle (for the diesel engine) is the topping cycle, and the Rankine cycle (for the RORC system) is the bottoming cycle. The performance of the combined system was evaluated using isopentane/R245fa as the working fluid.

Fig. 24(a) shows the improvement of power output by comparing the net power output of the combined system with the power output of just the diesel engine itself. As engine's speed and load increase, this improvement of power output gradually increases, although with some fluctuations in the trend. At the engine's rated condition, this improvement reaches a maximum of 10.54%. The calculating equation is:

$$\varphi_{ep} = \frac{\dot{W}_{net}}{\dot{W}_{en}} \times 100\% \tag{17}$$

The improvement of engine BSFC is shown in Fig. 24(b), which illustrates that there is a gradually increase in the improvement of engine BSFC (with some fluctuations) with increasing engine's speed and load. The improvement of engine BSFC reaches a maximum of 9.55% at the engine's rated condition. The BSFC of the combined system is calculated using

$$bsfc_{cs} = \frac{\dot{m}_{fu}}{\dot{W}_{cs}} \tag{18}$$

and the improvement of BSFC with

$$\varphi_{bf} = \frac{bsfc - bsfc_{cs}}{bsfc} \times 100\% \tag{19}$$

Since this prediction of overall BSFC improvement is based on some ideal assumptions, the result here is the maximum probable value corresponding to each operating condition of the diesel engine. Under real-world conditions, the BSFC improvement would be lower.

All the results are based on the assumption that the expander and heat exchangers always work in the ideal condition, so that we can evaluate the maximum potential of the RORC system. In order to propose a coordinated control theory for the combined engine and RORC system, the off-design behavior of the expander and heat exchangers will be investigated by we research group in the near future, similar to the research work mentioned in Ref. [35].

6. Conclusions

In this paper, the pure working fluid R245fa and the zeotropic mixture isopentane/R245fa were used in the RORC system, the performance of the RORC system was analyzed over the engine whole operating range. Then the performance of the combined engine and RORC system using the zeotropic mixture isopentane/R245fa was analyzed over the engine whole operating range. The conclusions are as follows:

1. The intermediate pressure and the fraction of steam extracted must be at a specific ratio in order to ensure that the working fluid is at a saturated liquid state at the outlet of the OFOH, and the fraction of steam extracted increases as the intermediate pressure increases.
2. The performance of the RORC system such as net power output, thermal efficiency, exergy efficiency, working fluid mass flow rate vary with the intermediate pressure for a given evaporating pressure. Therefore, the performance of the RORC system can be optimized by selecting a suitable intermediate pressure.
3. The optimal intermediate pressure for the zeotropic mixture of isopentane/R245fa is 1.15 MPa, while the optimal intermediate pressure for R245fa is 1.2 MPa. When using these respective pressures, the net power output, working fluid mass flow rate, and exergy destruction rate of the RORC system all increased with engine's speed and load, reaching their maximum values at the engine's rated condition. The exergy efficiency of the RORC system using the two different working fluids decreased with increasing engine speed and load, and reached its minimum at the engine's rated condition.

4. When isopentane is mixed with R245fa at a mole fraction ratio of 0.7/0.3, the mixture possesses the advantages of both pure working fluids, producing a larger net power output with a higher exergy efficiency but a lower mass flow rate and exergy destruction rate compared to pure R245fa.
5. Using an isopentane/R245fa mixture as the working fluid effectively increases the net power output and improves the BSFC. At the engine's rated condition, a 10.54% improvement in power output and a 9.55% improvement in fuel economy can be achieved.

Acknowledgments

This work was sponsored by the National Natural Science Foundation of China (Grant No. 51376011), Beijing Natural Science Foundation Program and Scientific Research Key Program of Beijing Municipal Commission of Education (Grant No. KZ201410005003), the National Basic Research Program of China (973 Program) (Grant No. 2011CB707202), the National High-Tech Research and Development Program of China (863 Program) (Grant No. 2009AA05Z206), Research Fund for the Doctoral Program of Higher Education of China (Grant No. 3C005015201301). The authors would like to appreciate Professor Chongfang Ma and Professor Yuting Wu for their great support during theoretical analysis process.

References

[1] Heywood JB. Internal combustion engine fundamentals. New York: McGraw-Hill, Inc.; 1988. p. 673–4.
[2] Dolz V, Novella R, García A, Sánchez J. HD diesel engine equipped with a bottoming Rankine cycle as a waste heat recovery system. Part 1: study and analysis of the waste heat energy. Appl Therm Eng 2012;36:269–78.
[3] Delgado-Torres Agustín M, García-Rodríguez Lourdes. Analysis and optimization of the low-temperature solar organic Rankine cycle (ORC). Energy Convers Manage 2010;51:2846–56.
[4] Wang JF, Yan ZQ, Wang M, Li MQ, Dai YP. Multi-objective optimization of an organic Rankine cycle (ORC) for low grade waste heat recovery using evolutionary algorithm. Energy Convers Manage 2013;71:146–58.
[5] Guo T, Wang HX, Zhang SJ. Selection of working fluids for a novel low-temperature geothermally-powered ORC based cogeneration system. Energy Convers Manage 2011;52:2384–91.
[6] Rentizelas A, Karellas S, Kakaras E, Tatsiopoulos I. Comparative techno-economic analysis of ORC and gasification for bioenergy applications. Energy Convers Manage 2009;50:674–81.
[7] Yu C, Chau KT. Thermoelectric automotive waste heat energy recovery using maximum power point tracking. Energy Convers Manage 2009;50:1506–12.
[8] Wei DH, Lu XS, Lu Z, Gu JM. Performance analysis and optimization of organic Rankine cycle (ORC) for waste heat recovery. Energy Convers Manage 2007;48:1113–9.
[9] Vaja I, Gambarotta A. Internal Combustion Engine (ICE) bottoming with organic Rankine cycles (ORCs). Energy 2010;35:1084–93.
[10] Katsanos CO, Hountalas DT, Pariotis EG. Thermodynamic analysis of a Rankine cycle applied on a diesel truck engine using steam and organic medium. Energy Convers Manage 2012;60:68–76.
[11] Shu GQ, Liu LN, Tian H, Wei HQ, Xu XF. Performance comparison and working fluid analysis of subcritical and transcritical dual-loop organic Rankine cycle (DORC) used in engine waste heat recovery. Energy Convers Manage 2013;74:35–43.
[12] Bombarda P, Invernizzi CM, Pietra C. Heat recovery from diesel engines: a thermodynamic comparison between Kalina and ORC cycles. Appl Therm Eng 2010;30:212–9.
[13] Srinivasan KK, Mago PJ, Krishnan SR. Analysis of exhaust waste heat recovery from a dual fuel low temperature combustion engine using an organic Rankine cycle. Energy 2010;35:2387–99.
[14] Boretti A. Recovery of exhaust and coolant heat with R245fa organic Rankine cycles in a hybrid passenger car with a naturally aspirated gasoline engine. Appl Therm Eng 2012;36:73–7.
[15] Acar Hİ. Second law analysis of the reheat-regenerative Rankine cycle. Energy Convers Manage 1997;38:647–57.
[16] Mago PJ, Chamra LM, Srinivasan K, Somayaji C. An examination of regenerative organic Rankine cycles using dry fluids. Appl Therm Eng 2008;28:998–1007.
[17] Wang EH, Zhang HG, Fan BY, Wu YT. Optimized performances comparison of organic Rankine cycles for low grade waste heat recovery. J Mech Sci Technol 2012;26:2301–12.
[18] Zhang HG, Wang EH, Fan BY. Heat transfer analysis of a finned-tube evaporator for engine exhaust heat recovery. Energy Convers Manage 2013;65:438–47.
[19] Fiaschi D, Manfrida G, Maraschiello F. Thermo-fluid dynamics preliminary design of turbo-expanders for ORC cycles. Appl Energy 2012;97:601–8.
[20] Li J, Pei G, Li Y, Ji J. Evaluation of external heat loss from a small-scale expander used in organic Rankine cycle. Appl Therm Eng 2011;31:2694–701.
[21] Wang TY, Zhang YJ, Peng ZJ, Shu GQ. A review of researches on thermal exhaust heat recovery with Rankine cycle. Renew Sustain Energy Rev 2011;15:2862–71.
[22] Bao JJ, Zhao L. A review of working fluid and expander selections for organic Rankine cycle. Renew Sustain Energy Rev 2013;24:325–42.
[23] Mujic E, Kovacevic A, Stosic N, Smith I. Advanced design environment for screw machines; 2010.
[24] Leibowitz H, Smith IK, Stosic N. Cost effective small scale ORC systems for power recovery from low grade heat sources. IMECE2006-14284.
[25] Wang W, Wu YT, Ma CF, Liu LD, Yu J. Preliminary experimental study of single screw expander prototype. Appl Therm Eng 2011;31:3684–8.
[26] Wang EH, Zhang HG, Fan BY, Ouyang MG, Zhao Y, Mu QH. Study of working fluid selection of organic Rankine cycle (ORC) for engine waste heat recovery. Energy 2011;36:3406–18.
[27] Wang JL, Zhao L, Wang XD. An experimental study on the recuperative low temperature solar Rankine cycle using R245fa. Appl Energy 2012;94:34–40.
[28] Rayegan R, Tao YX. A procedure to select working fluids for solar organic Rankine cycles (ORCs). Renew Energy 2011;36:659–70.
[29] Tchanche BF, Papadakis G, Lambrinos G, Frangoudakis A. Fluid selection for a low-temperature solar organic Rankine cycle. Appl Therm Eng 2009;29:2468–76.
[30] Garg P, Kumar P, Srinivasan K, Dutta P. Evaluation of isopentane, R-245fa and their mixtures as working fluids for organic Rankine cycles. Appl Therm Eng 2013;51:292–300.
[31] Lemmon EW, Huber ML, McLinden MO. NIST standard reference data base 23: reference fluid thermodynamic and transport properties-REFPROP, Version 9.0, National Institute of Standards and Technology, Standard Reference Data Program, Gaithersburg; 2010.
[32] Zhang HG, Wang EH, Fan BY. A performance analysis of a novel system of a dual loop bottoming organic Rankine cycle (ORC) with a light-duty diesel engine. Appl Energy 2013;102:1504–13.
[33] Florian H, Markus P, Dieter B. Zeotropic mixtures as working fluids in organic Rankine cycles for low-enthalpy geothermal resources. Renew Energy 2012;37:364–70.
[34] MATLAB version 7.12.0.635 (R2011a). Matlab user's guide. US: The Mathworks Inc.; 2011.
[35] Wang JF, Yan ZQ, Zhao P, Dai YP. Off-design performance analysis of a solar-powered organic Rankine cycle. Energy Convers Manage 2014;80:150–7.